World Conference on Timber Engineering Oslo 2023

COMPONENT METHOD IN TIMBER CONNECTIONS: END-PLATE COMPRESSING TIMBER PARALLEL TO GRAIN COMPONENT STRENGTH

Arthur S. Rebouças[1], Jorge M. Branco[2], Paulo B. Lourenço[3], Hidelbrando J. F. Diógenes[4]

ABSTRACT: The component method considers the whole joint as a set of individual basic components, dividing them into zones of tension, compression, and shear. The strength of end-plate and timber parallel to grain in compression may influence total resistance and failure mode of the joint. The objective of this work is to characterize the strength of the component corresponding to a glulam beam under compression by an end-plate in bending within an application in moment-resisting timber connections. For this, an experimental campaign was conducted through compression tests on 25 specimens composed of steel T-stubs with five different flange thicknesses and glulam GL24h. The results were compared to reference compression tests using a rigid plate. A decrease in the component resistance was observed with the reduction in the flange thickness. The failure of the component was governed by the T-stub, due to flange yielding, while the timber did not show characteristic failure. Based on the Eurocode 3 equivalent plate concept, an approach with variable stress distribution was proposed, it proved to be coherent with the experimental behavior of the component and with a possible application in design since the analytical values maintain an acceptable safety margin in relation to the experimental ones.

KEYWORDS: Timber connections, Component method, Glulam beam in compression, End-plate in bending.

1 COMPONENT METHOD

One of the current design practices to predict the rotational behavior of steel joints adopted by EN 1993-1-8 [1] is based on the component method, an analytical method that considers the whole joint as a set of individual basic components, dividing them into zones of tension, compression and shear. It allows to obtain the design moment resistance, rotation capacity, initial and post-peak stiffness and built a moment-rotation curve using these data [2]. The application of component method provides a tri-linear moment-rotation curve to characterize a connection and requires the following steps:

I. Identification of the active/relevant components in the joint being considered;
II. Evaluation of the stiffness and/or resistance characteristics for each individual basic component (specific characteristics – initial stiffness, design resistance, … – or whole deformability curve);
III. Assembly of all the constituent components and evaluation of the stiffness and/or resistance characteristics of the whole joint (specific characteristics – initial stiffness, design resistance, … – or whole deformability curve).

The relevant components are the ones that transfer significant internal forces based on the joint behavior. Each of these basic components possesses its own strength and stiffness either in tension, compression or shear. The coexistence of several components within the same joint element can obviously lead to stress interactions that are likely to decrease the resistance of the individual basic components.

A large amount of research in the field of steel structures was conducted applying the component method to mechanical analysis of steel joints, since Zoetemeijer [3] and Jaspart [4] until more recent studies for cyclic loading [5] and other geometries [6]. From the recognition of the reliability and relevance of the component method to characterize steel joints, some research was conducted in several types of timber connections: historical [7], slotted-in steel plates [8], glued-in rods [9,10] and glued-in steel plates [11]. On the other hand, despite a considerable part of the timber joints using steel components, the effectiveness of the component method in the analysis of timber joints has not been fully assessed.

Therefore, the objective of this work is to characterize the strength of the component corresponding to a glulam beam under compression by an end-plate in bending within an application in moment-resisting timber connections.

[1] Arthur S. Rebouças, Federal Institute of Education, Science and Technology of Rio Grande do Norte, IFRN, Brazil & Department of Civil Engineering, University of Minho, ISISE, Portugal, arthur.reboucas@ifrn.edu.br
[2] Jorge M. Branco, Department of Civil Engineering, University of Minho, ISISE, Portugal, jbranco@civil.uminho.pt
[3] Paulo B. Lourenço, Department of Civil Engineering, University of Minho, ISISE, Portugal, pbl@civil.uminho.pt
[4] Hidelbrando J. F. Diógenes, Federal University of Paraíba, PPGECAM, Brazil, hjfd@academico.ufpb.br

https://doi.org/10.52202/069179-0038

2 GLULAM BEAM IN COMPRESSION AND END-PLATE IN BENDING

Tomasi et al. [12] and Andreolli et al. [9] modelled the glulam beam and the end-plate/steel profile flange in compression as equivalent T-stub in compression. In the connection studied by them (Figure 1), there is a direct contact between the end-plate and the glulam along the total joint depth. In this approach, the effective area of compression plays an important role, as it is directly related to the compressive resistance and stiffness of the component. In these studies, the compressive area was proposed according to EN 1993-1-8 [1], considering that the compression stress is uniformly distributed over a rectangular area measuring by an effective length ($l_{eff,c}$) and width ($b_{eff,c}$), as shown in Figure 2. These dimensions can be taken by the additional bearing width (c_t), which was also calculated based on the EN 1993-1-[1] with some adaptations (Equation 1). The glulam beam compression strength was determined by Equation 2.

$$c_t = t_{ep}\sqrt{\frac{f_y}{3 \cdot f_{c,0} \cdot \gamma_{M0}}} \quad (1)$$

$$F_{R,gb,c} = f_{c,0,d} \cdot b_{eff,c} \cdot l_{eff,c} \quad (2)$$

Where, t_{ep} [mm] is the thickness of end-plate, f_y [N/mm²] is the yield strength of steel, $f_{c,0}$ [N/mm²] is the compression strength parallel to grain of the glulam beam, and γ_{M0} [unitless] is the coefficient equal to 1.

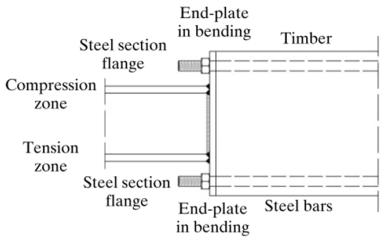

Figure 1. *Connection studied by Tomasi et al. [12] and Andreolli et al. [9].*

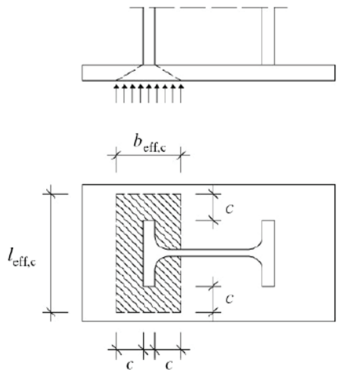

Figure 2. *Compressive area defined in Tomasi et al. [12] and Andreolli et al. [9].*

Yang et al. [10] and Tao et al. [11] applied the procedure proposed by [9] to calculate the resistance of glulam beam in compression parallel to the grain. In these studies, the timber beam is under compression by a steel plate which structural behavior can be modelled as an equivalent T-stub. In the connection studied by Yang et al. [10] (Figure 3), there is a contact area between the steel box and timber beam, where both are under compression. As the steel box width is equal to the glulam beam width, the effective compression area of glulam beam was defined as shown in Figure 4. The effective width was defined as equal to the glulam width (b_b) and the effective bearing length was taken as $0.5 \cdot h_{srt}$. However, no additional explanation was given on how to obtain these values. The glulam beam compression resistance was determined by Equation 3.

$$F_{R,gb,c} = f_{c,0} \cdot b_b \cdot 0.5 \cdot h_{srt} \quad (3)$$

Where b_b [mm] is the width of glulam beam and h_{srt} [mm] is the cross-sectional depth of the steel box.

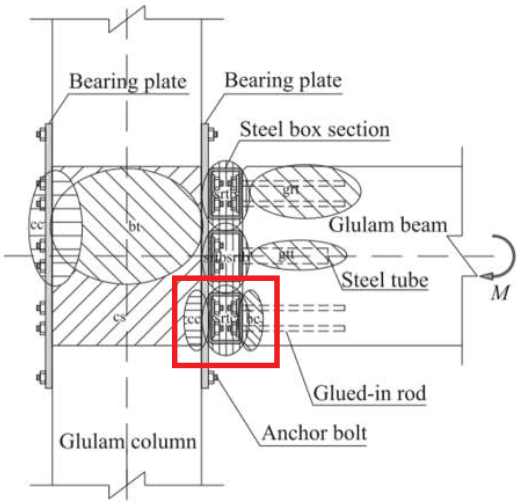

Figure 3. *Compression sub-region in the bottom of connection Adapted from [10].*

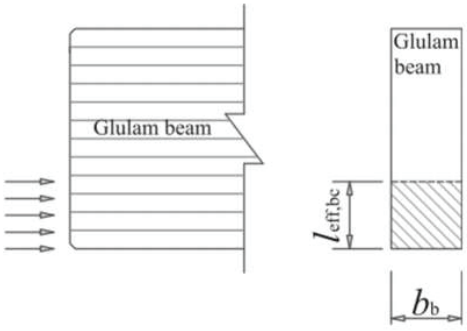

Figure 4. *Effective compression area of glulam beam. Adapted from [10].*

Nevertheless, the c_t and $F_{R,gb,c}$ mentioned above were determined from an adaptation of [1] for the component called "base plate and concrete block in compression". According to Steenhius et al. [13] this component is a base

https://doi.org/10.52202/069179-0038

plate, assumed to be flexible in bending and modelled as a T-stub in compression, supported by a concrete block in compression, with stresses concentrated around the footprint of the column section under the plate. Stockwell [14], Murray [15] and Steenhuis and Bijlaard [16] introduced the concept of replacing a flexible plate with a non-uniform stress distribution by an equivalent rigid plate with a uniform stress distribution, later added to Eurocode 3 (Figure 5).

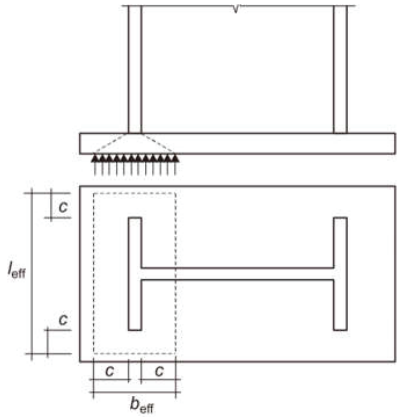

Figure 5. *Effective area of T-stub in compression [1]*

The resistance of the component is determined by two parameters: the bearing strength of the concrete and the dimensions of the equivalent rigid plate. The design compression resistance of the component $F_{C,Rd}$ and the maximum additional bearing width c is defined in the EN 1993-1-8 [1], section 6.2.5, as shown in Equations 4 and 5, respectively.

$$F_{C,Rd} = f_{jd} \cdot b_{eff} \cdot l_{eff} \quad (4)$$

$$c = t\sqrt{\frac{f_y}{3 \cdot f_{jd} \cdot \gamma_{M0}}} \quad (5)$$

Where b_{eff} [mm] is the effective width of the T-stub flange; l_{eff} [mm] is the effective length of the T-stub flange; t [mm] is the thickness of the T-stub flange; f_y [N/mm²] is the yield strength of the T-stub flange and f_{jd} [N/mm²] is the design bearing strength of the joint. It should be determined from Equation 6.

$$f_{jd} = \frac{\beta_j \cdot F_{Rdu}}{b_{eff} \cdot l_{eff}} \quad (6)$$

Where β_j [unitless] is the foundation joint material coefficient, which may be taken as 2/3 provided that the characteristic strength of the grout is not less than 0.2 times the characteristic strength of the concrete foundation and the thickness of the grout is not greater than 0.2 times the smallest width of the steel base plate. In cases where the thickness of the grout is more than 50 mm, the characteristic strength of the grout should be at least the same as that of the concrete foundation; F_{Rdu} [N/mm²] is the concentrated design resistance force given in EN 1992-1-1 (2014), here in Equation 7.

$$F_{Rdu} = A_{c0} \cdot f_{cd} \quad (7)$$

Where A_{c0} [mm²] is the loaded area, here equal to $b_{eff} \cdot l_{eff}$.

Therefore, it is possible to identify, by comparing the Equations 4, 5 and 7 with 1, 2 and 3 ones, that the formulation used by [9] and [12] is very close to the one used to concrete block in compression. For the resistance and the additional bearing width, it differs only by the strength of the material used.

It is believed that this approach needs some adaptations, since the deformation of a glulam beam under compression by a steel plate (equivalent T-stub) can be much pronounced than that seen in a concrete block. It also directly influences the computation of effective area in the equivalent rigid plate.

3 EXPERIMENTAL CAMPAIGN

An experimental campaign was conducted through compression tests on 25 specimens composed of steel T-stubs, with five different flange thicknesses (6, 8, 10, 15 and 20mm), connected to glued laminated timber specimens. The results were compared to reference compression tests using a rigid plate with thickness equal to 40mm, these specimens are regular plates, not T-stubs. Five tests were made for each group.

3.1 SPECIMENS

As timber elements, glulam made of spruce (*Picea abies*) from strength class GL24h, according to EN 14080:2013 [17], were used. As steel elements, T-stub specimens of steel S235, with yield strength equal to 235N/mm² and ultimate tensile strength of 360N/mm², according to the EN 1993-1-1:2010 [18] were applied. The timber specimens had the same dimensions for all test series, 120×240×240mm³. T-stubs geometry are similar (Figure 6), only the thickness varies, as presented in Table 1. The name of each series was defined as "T' plus its corresponding thickness and the reference one was called "REF". The front face of each specimen was painted to be adequate to DIC measurements, the detailed information about the whole configuration is presented in Figure 7. A summary of T-stub and timber specimens tested can be found in Table 1.

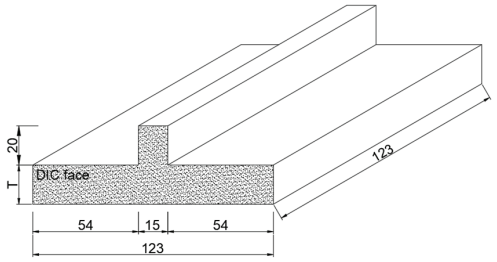

Figure 6. *T-stub specimens dimensions (mm)*

https://doi.org/10.52202/069179-0038

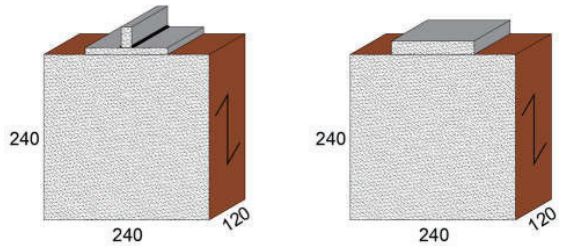

Figure 7. *Detailed geometry of the specimens, including T-stub and glulam, the DIC painted front face and positions of (a) T-stub specimens and (b) Reference specimens. Dimensions in mm.*

Table 1: *Summary of the steel and timber specimens tested, including the reference group (each series comprehends 5 specimens).*

Series	Steel specimens		Timber specimens	
	T-stub flange thickness [mm]	Plate thickness [mm]	Geometry [mm]	
			Cross section	Height
REF	-	40	120×240	240
T20	20	-	120×240	240
T15	15	-	120×240	240
T10	10	-	120×240	240
T8	8	-	120×240	240
T6	6	-	120×240	240

3.2 TEST METHOD

The compression tests of the specimens were carried out on a hydraulic jack with a load cell of 1500 kN under displacement control at a rate of 3 mm/min. The load was applied along the center part of T-stub. The tests were finished when the force reached 80% of the maximum force or when the central displacement reached 2,5% of the specimen total height. The vertical displacements were monitorized by three LVDTs positioned according to the Figure 8, as follows: the central one measured the total displacement of glulam specimen; the left and right ones measured the displacement from each T-stub edge to the glulam specimen. The 3D displacements, deformations, and local strains on the surface between the two materials were determined by the Digital Image Correlation (DIC). In the scope of this work, INSTRA 4D V4.4.7 x64 software was used along with two cameras (Master and Slave) of 2.0 megapixels positioned 100 cm between each other. The acquisition frequency to obtain the frames was 1 Hz.

Figure 7. *Positions of displacement transducers. The right and left ones were named based on the front face of the specimen (painted face).*

3.3 RESULTS

The average maximum experimental stress of the "REF" series was 33.35 MPa, 38.95% higher than the 24 MPa guaranteed by the manufacturer. For the other series, measuring the experimental stress applied by the T-stub flange on timber is complex, due to the lifting of the T-stub flange edges, there is a gradual reduction in the contact area between the two materials. Therefore, the resistance of the component can be better characterized in terms of force.

The Figure 9 shows the force-displacement curves, measured from the center transducer data for tests with average response in each thickness range. In the results of the series "REF" the force decreased gradually after maximum point, whereas for all other series, the force stayed on a plateau with a large increase in displacement. In general, a decrease in the maximum force was observed with the reduction in the thickness of the flange.

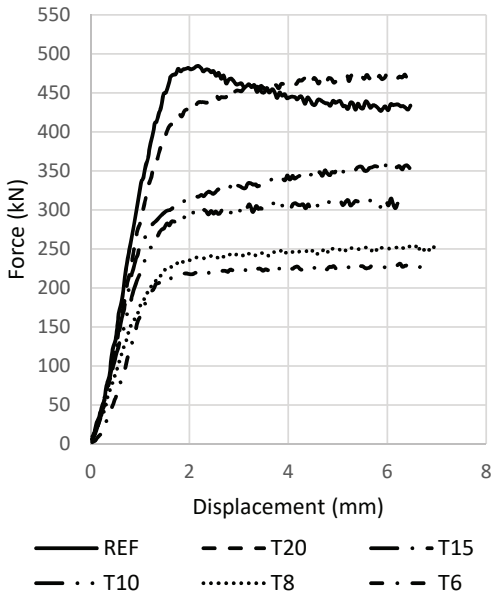

Figure 9: *Force-displacements curves for all different T-stub flange thicknesses.*

https://doi.org/10.52202/069179-0038

In all series, there was a greater displacement of the center of the T-stub flange in relation to the ends, from the beginning of the test. For example, this bending can be seen in the Figure 10, that shows the deformed shape of the T15 specimen when the maximum force was achieved.

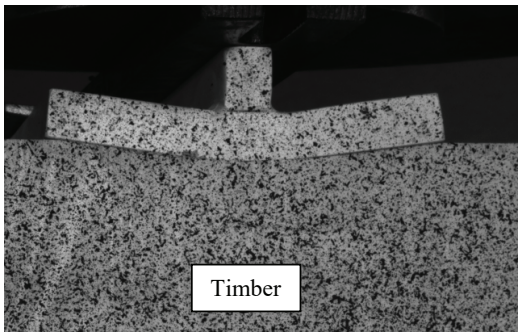

Figure 10: *Deformed shape of specimen T15-E4 at maximum force.*

The smaller the thickness of the flange, the greater was this difference in displacement between center and edges. For thicknesses of 10, 8 and 6 mm, a negative displacement was observed (the position of the end of the plate was smaller than its position at the beginning of the test), an example is shown in Figure 11.

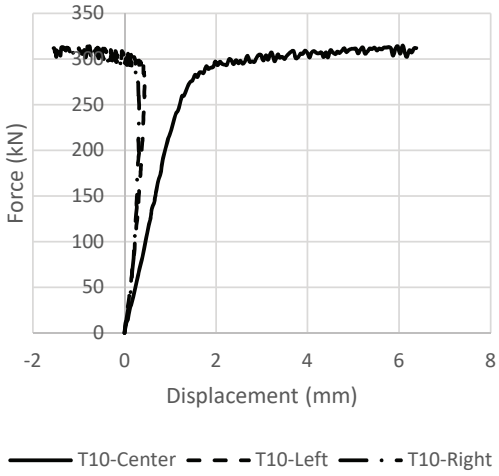

Figure 11: *Force-displacements curve for T10-E4.*

In all tests, the failure of the component was governed by the T-stub, due to the excessive displacement of its edges, without rupture (T-stub flange yielding), while the timber did not show characteristic failure (Figure 12). Except for "REF" series, which the timber presented local failure due to compression under the loading plate (Figure 13).

Figure 12: *Failure of specimen T6-E3 due to T-stub flange yielding.*

Thus, the component experimental behavior is based on identifying whether the stress applied by the T-stub to the timber is sufficient to reach the compressive strength parallel to the grain before reaching the plastic resistant moment of its flange. In all cases studied, although the elastic limit of timber has been clearly reached (see Figures 9 and 11), the compressive strength of the timber was not achieved, therefore, all T-stub flanges can be considered flexible.

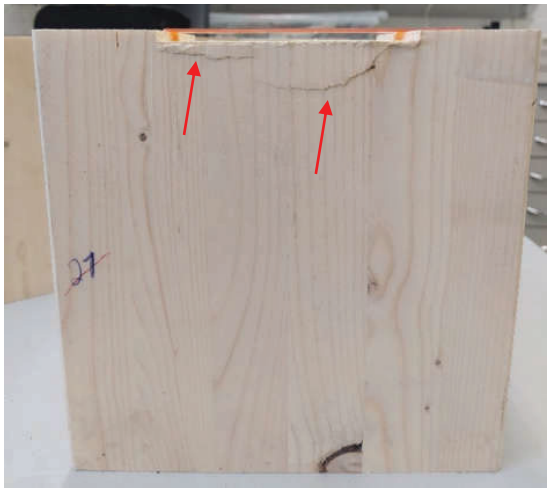

Figure 13: *Deformed shape of specimen T15-E4 at maximum force.*

The component strength based on the formulation proposed by Andreolli et al. [9] was assessed, considering the elastic moment resistance of the T-stub flange and the average maximum experimental stress of the "REF" series (33.35 MPa), as timber strength. It was identified,

from the DIC measurements, that the T-stub flanges are still below the steel yield strain limit for all tested series. The displacements in timber and steel when the force applied was equal to the component strength found by [9] proposition are shown in Figure 14. The strain values were obtained from the vertical displacement and the applied force.

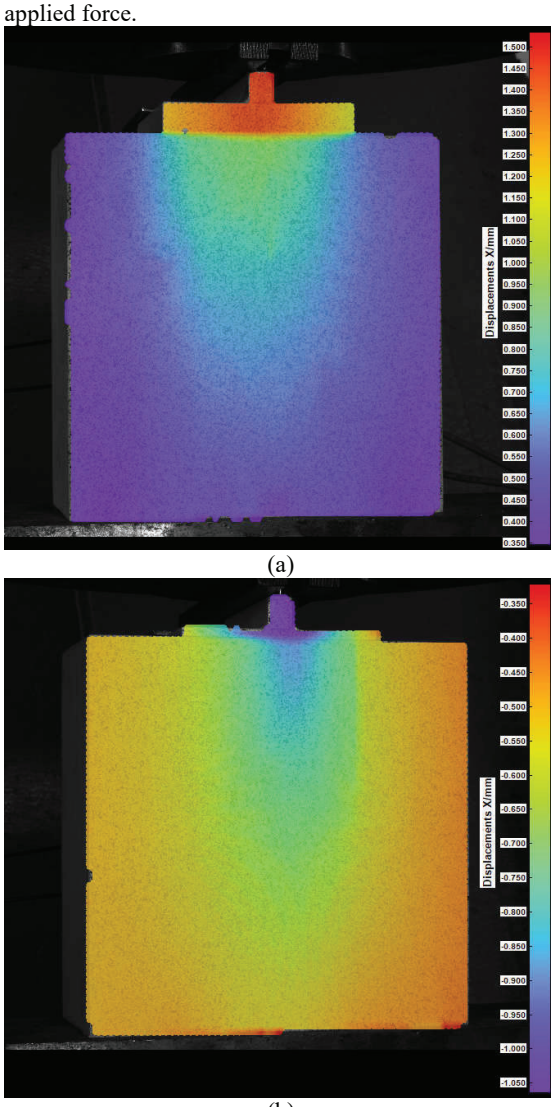

Figure 14: *Displacements registered through Digital Image Correlation for (a) T20 (b)T6.*

4 COMPONENT RESISTANCE PROPOSALS

4.1 PLASTIC RESISTANCE OF STEEL

The plastic bending moment resistance of the base plate per unit length should be taken as presented in Equation 8.

$$M_{pl} = \frac{1}{4} t_{ep} \cdot f_y \qquad (8)$$

Each side of T-stub was modeled as a cantilever beam and a uniform stress distribution in the contact between the plate and the timber was considered (Figure 15). According to the equivalent plate theory, equaling the plastic bending moment resistance of the base plate to a bending moment on the plate, Equation 9 is obtained to determine the equivalent bearing width. The resistance of the component can be obtained from the equivalent area, but in this case using the plastic additional bearing width (c_{tp}).

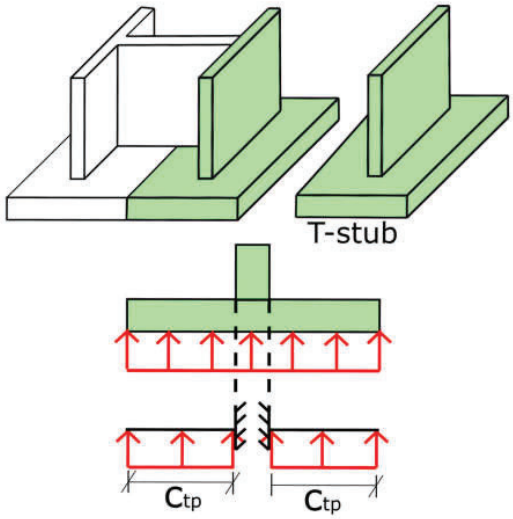

Figure 15. *Structural idealization of the component corresponding to the steel T-stub applying compression parallel to grain in timber member.*

$$c_{tp} = t_{ep} \sqrt{\frac{f_y}{2 \cdot f_{c,0} \cdot \gamma_{M0}}} \qquad (9)$$

4.2 VARIABLE STRESS DISTRIBUTION

From the DIC measurements, it was observed that, as expected, there is a non-uniform distribution of displacements in the contact between the steel plate and the timber. As shown in Figure 16(a), the displacements around the central part of the T-stub are greater, reducing towards the edges. This was repeated in all test types and for all plate thicknesses, since the beginning of the compression application. Based on those observations, a new approach is proposed for determining the equivalent bearing width, considering a variable distribution of stresses in contact between both materials, as shown in Figure 16(b).

https://doi.org/10.52202/069179-0038

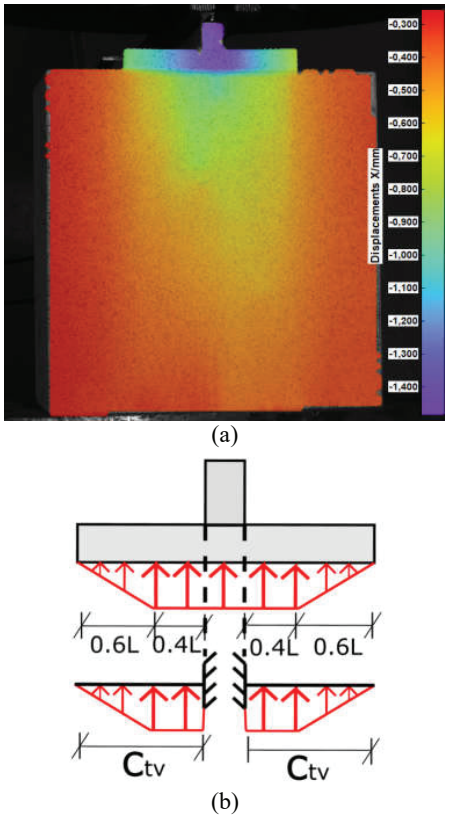

Figure 16. *(a) General displacements distribution from DIC tests. (b) Structural idealization for T-stub and timber in compression component with variable stress distribution.*

Considering this new stress distribution, the maximum moment acting on the T-stub becomes equal to $0.26 \cdot q \cdot L^2$ and, assuming the plate in elastic range, the Equation 10 can be formulated to calculate the c_{tv}. The component strength can be obtained from the equivalent area using variable distribution additional bearing width (c_{tv}).

$$c_{tv} = t_{ep}\sqrt{\frac{f_y}{1.56 \cdot f_{c,0} \cdot \gamma_{M0}}} \qquad (10)$$

5 RESULTS AND DISCUSSION

For simplicity in discussion of the results, the following nomenclatures were given for the propositions: Andreolli's one was called uniform distribution in elastic range (UD-ER), the plastic bending preposition was uniform distribution in plastic range (UD-PR) and the variable stress distribution was VD-ER. The analytical values of the component strength were calculated computing the $f_{c,0}$ equal to 24 MPa.

In Figure 17, it is possible to observe the curves of the relative displacements between the center and the edges of the T-stub flanges of two tests and in Table 2 the average strains for all the tests carried out. It appears that even considering the plastic limit of steel (UD-PR) or the variable stress distribution (VD-ER), the T-stub seems to be in a safe region from the design point of view, since the highest analytically determined strength is approximately 70% for specimen T20 and 55% for specimen T6 in relation to the experimental component strength.

As it is the T-stub that governs the structural behavior of the component, the strength reserve and ductility of steel can be exploited.

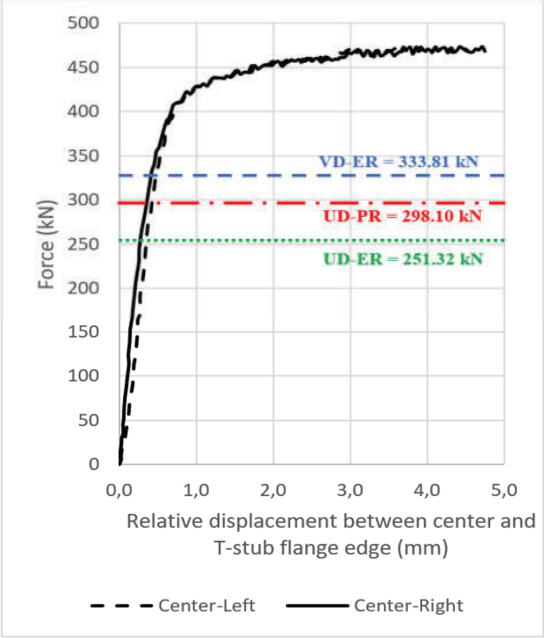

(a)

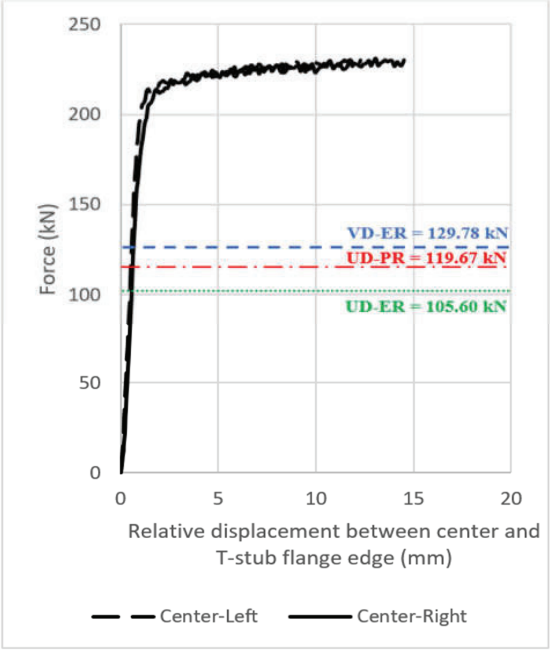

(b)

Figure 17: *Force-relative displacements curves for (a) T20 GT2 (b) T6 GT2.*

Table 2: *Summary of the steel and timber specimens tested, including the reference group.*

		UD-ER	UD-PR	VD-ER
T20	Force (kN)	251,32	298,10	331,81
	Relative Displac. (mm)	0,36	0,45	0,53
	Strain	0,0025%	0,0039%	0,0053%
T15	Force (kN)	199,29	234,37	259,66
	Relative Displac. (mm)	0,38	0,50	0,62
	Strain	0,0027%	0,0046%	0,0072%
T10	Force (kN)	147,26	170,65	187,51
	Relative Displac. (mm)	0,47	0,55	0,62
	Strain	0,0042%	0,0056%	0,0073%
T8	Force (kN)	126,45	145,16	158,65
	Relative Displac. (mm)	0,62	0,75	0,87
	Strain	0,0073%	0,0107%	0,0144%
T6	Force (kN)	105,60	119,67	129,78
	Relative Displac. (mm)	0,60	0,67	0,75
	Strain	0,0074%	0,0088%	0,0111%

The Figure 18 shows the maximum experimental component resistances and the theoretical values obtained by the three presented approaches: UD-ER, UD-PR and VD-ER. The proposals are coherent compared to the experimental tests. The bearing capacity of test specimens at T-stub failure is in the range from 1.36 (T20) to 1.88 (T6) times the capacity calculated according to variable distribution proposal, considering the average of experimental component strength. An improvement in the accuracy of the results was identified, since for UD-ER approach, the values were 1.80 (T20) and 2.31 (T6). In addition, the use of a variable distribution in elastic range (VD-ER), with greater displacements in the central region of the T-stub, is more consistent with the experimental behavior of the component.

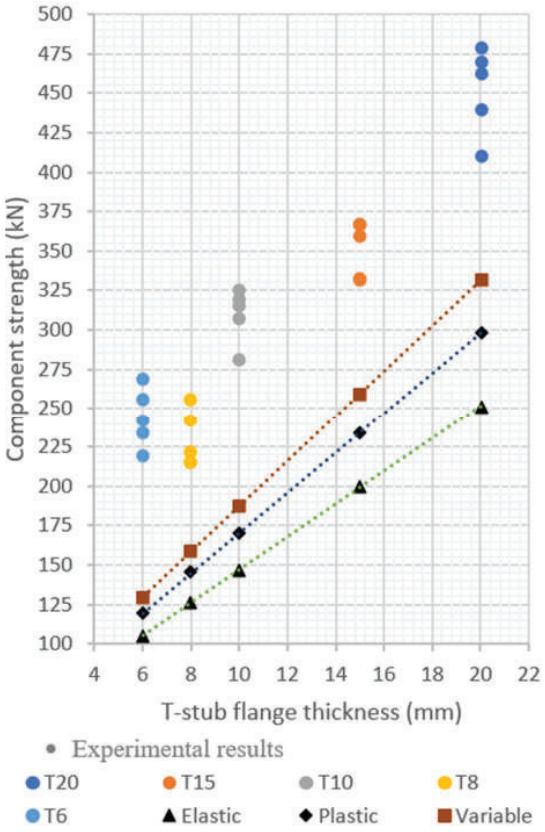

Figure 18: *Maximum component experimental resistances and theoretical values for the three different proposals.*

6 CONCLUSIONS

The structural behavior of the end-plate compressing timber parallel to grain component is governed by the yielding of the T-stub flange, for thicknesses usually used in design. In all compression tests, the timber did not show a clear and well-characterized failure, as occurred in the reference tests with a rigid plate.

As the stresses transmission is carried out by the contact between the two materials and according to the T-stub stiffness, the component strength is proportional to the thickness of the plate, that is, the greater the thickness of the plate, the greater the component strength.

From the beginning of each test, there is a difference in displacements between the central part and the edges of the T-stub flange, which indicates the occurrence of a non-uniform stress distribution between the T-stub flange and the timber. To analytically evaluate and predict the component strength, the concept of equivalent rigid plate was used, but in three different approaches.

The proposition of the equivalent plate with variable stress distribution proved to be coherent with the experimental behavior of the component and with a possible application in design, since the analytical values maintain an acceptable safety margin in relation to the experimental ones.

https://doi.org/10.52202/069179-0038

ACKNOWLEDGEMENT

Thanks to the Fundação para a Ciência e Tecnologia (FCT) for supporting this research under grant number BD/06301/2021. The work is part of RILEM TC TPT "Tests methods for a reliable characterization of resistance, stiffness and deformation properties of timber joints".

REFERENCES

[1] EN 1993-1-8 Eurocode 3: Design of steel structures - Part 1-8: Design of joints, European Committee for Standardisation, 2012

[2] J.-P. Jaspart, K. Weynand, Design of Joints in Steel and Composite Structures, ECCS Press/Ersnest & Sohn, 2016.

[3] P. Zoetemeijer, A design method for the tension side of statically loaded, bolted beam-to-column connections, HERON 20, 1974.

[4] J.-P. Jaspart, General report: session on connections, J. Constr. Steel Res. 55, 2000.

[5] Oliveira S., Costa R., Shahbazian A., Rebelo C., Harada Y., Simões da Silva L.: Component-based method for quasi-static cyclic behaviour ofsteel joints. Journal of Constructional Steel Research, 181, 2021.

[6] Wan W., Yan S., Zhang H, Rasmussen K.J.R.: A generalised component method for bolted angle connections. Journal of Constructional Steel Research, 2022.

[7] Wald F., Mares J., Sokol Z.: Component method for historical timber joints. The Paramount Role of Joints into the Reliable Response of Structures, 417-424, 2000.

[8] Postupka J., Kuhlmann U., Brühl F.: Ductile behaviour of dowl connections – application of the component method in timber construction. WCTE 2016

[9] Andreolli, M., Piazza, M., Tomasi, R., & Zandonini, R.: Ductile moment-resistant steel-timber connections. Proceedings of the Institution of Civil Engineers: Structures and Buildings, 164(2), 65–78, 2011.

[10] Yang, H., Liu, W., & Ren, X.: A component method for moment-resistant glulam beam-column connections with glued-in steel rods. Engineering Structures, 115, 42–54, 2016.

[11] Tao, H., Mao, M., Yang, H., & Liu, W.: Theoretical and experimental behaviour of a hybrid semi-rigid glulam beam-to-column connection with top and seat angles. Advances in Structural Engineering, 23(10), 2057–2069, 2020.

[12] Tomasi, R., Zandonini, R., Piazza, M., & Andreolli, M.: Ductile end connections for glulam beams. Structural Engineering International: Journal of the International Association for Bridge and Structural Engineering (IABSE), 18(3), 290–296, 2008.

[13] Steenhuis, M., Wald, F., Sokol, Z., Stark, J.: Concrete in compression and base plate in bending HERON Vol. 53, No ½, 2008.

[14] Stockwell, F.W. Jr. Preliminary Base Plate Selection, Engineering Journal AISC, Vol. 21, No.3, 1975, pp. 92-99.

[15] Murray T.M. Design of Lightly Loaded Steel Column Base Plates, Engineering Journal AISC, Vol. 20, 1983, pp. 143-152.

[16] Steenhuis, C.M., Bijlaard F. S. K. Tests On Column Bases in Compression, Published in the Commemorative Publication for Prof. Dr. F. Tschemmemegg, ed. by G. Huber, Institute for Steel, Timber and Mixed Building Technology, Innsbruck 1999.

[17] EN 14080: Timber structures - Glued laminated timber and glued solid timber - Requirements, European Committee for Standardisation, 2013.

[18] EN 1993-1-1 Eurocode 3: Eurocode 3: Design of steel structures - Part 1-1: General rules and rules for buildings, 2012.